

A Monte-Carlo Approach for Modeling Glass Transition

H. H. Ruan and L. C. Zhang[†]

School of Mechanical & Manufacturing Engineering, The University of New South Wales, Sydney, NSW, 2052, Australia

Glass transition is an important factor in the thermo-forming of glass elements of precision geometries, such as optical glass lenses. Based on the theory of potential energy landscape, the master equations can be established to describe the slowdown of atomic motions in the glass transition range. However, the direct solution of these master equations is almost formidable as the hopping rates between basins vary in many orders of magnitude. To make use of the master equations in the finite element simulation of thermo-forming process, this article develops a Metropolis stochastic process by assuming that the basin-hopping probability at a given time interval depends only on the relative hopping rate between the target state and the present state. It was shown that with an infinitesimal time interval, this stochastic description degenerates to the master equations, and that with coarse time steps, the efficiency can be greatly improved with good accuracy. The advantage of this new method was demonstrated through the glass transition and thermo-forming simulations of selenium by integrating the stochastic process with the finite element method *via* the constitutive description of the variation of volume and viscosity with temperature and time.

I. Introduction

Glass transition is the oldest and most important thermodynamic process in the production of glass articles. Even in the ancient times, a skillful artisan could create glass objects of diverse and pleasing shapes by manipulating the temperature-dependent fluidity of glass. However, in applying the same process to produce high-precision glass elements, for example, optical lens¹ or mechanical parts,² there exist significant difficulties in the control of many key aspects associated with the shaping of glass, such as geometry, density, residual stress, and refractive index.³ In a sense, all these difficulties are due to the limited understanding of the underlying physics of glass transition.⁴

The phenomenology of glass transition is the continuous change of thermodynamic variables, such as volume or enthalpy, with temperature and time. Different cooling rates lead to different properties of a glass material. Such dependency can be delineated by the well-known phenomenological model proposed by Tool⁵ and Narayanaswamy,⁶ who ascribed the glass transition to the superposition of the temperature-dependent exponential or nonexponential relaxation processes with the parameters determined by fitting experimental relaxation of some instantaneously measurable variables, for example, the refractive index.⁷ Although this model seems straight and easily implementable, it does not offer insight into the physics of the glass transition. It is also questionable to use the parameters thus obtained to the variables not instantaneously measurable.

To involve the insight of microscopic structure in the theoretical model of amorphous material, Turnbull, Cohen, and Grest^{8,9} considered that the volumetric difference between the randomly packed and the orderly packed atomic systems was a key variable in distinguishing glass and crystal. The ensemble average of this volume difference was termed the free volume. Free volume can nucleate and diffuse in materials and act like dislocation in crystals to induce change of atomic structures and affect the fluidity of a supercooled liquid.^{10,11} This single-variable theory is preferred in many research works. However, its application is limited due to its oversimplification.¹² Mode-coupling theory^{13,14} is another approach in distinguishing the supercooled liquids from equilibrium liquids, which predicts the occurrence of solid-like atomic structure with long relaxation time (alpha-relaxation). However, its applicability is also limited to the high-temperature regime far from the glass transition regime. Direct molecular dynamics (MD) simulation is a powerful tool; but due to its extremely short integration time step (typically a femtosecond),¹⁵ it can only handle nanoscale problems with unrealistically fast cooling process.

A significant pace in understanding glass transition has been made by the theory of the potential energy landscape (PEL) introduced by Goldstein¹⁶ and Stillinger and Webber.^{17,18} It was envisaged that the potential energy variation over the space of atomic coordinates is a hyper-surface with wells, peaks, and saddles. The basic idea was to characterize this hyper-surface by two features, namely, the energy minima, corresponding to the mechanically stable packings, named inherent structures, and the basins surrounding the energy minima, corresponding to the vibration motion about those mechanically stable points. As the inherent structure is generally considered temperature-independent, the vibration motion is thermally activated which renders the probability for system hopping between inherent structures. It is reasonable to assume that many physical properties depend merely on how the atoms are packed. Therefore, if one knows such dependency and probabilities for the system to take each of the inherent structures, the macroscopic property, based on the ensemble theory, will be a simple calculation of the statistical expectation. Heuer¹⁹ has provided an excellent review of the PEL theory.

As the exploration of all potential energy minima is formidable even for tens of atoms, the application of the PEL theory requires further simplification. The most striking assumption has been that similar inherent structures with very close energy minima can be visited with the same probability therefore can be grouped as the same microstate, or the basin.²⁰ The number of the distinct atomic arrangements in each basin can be regarded as the degeneracy, which may be determined from the equilibrium state¹⁹ or by the Wang–Landau algorithm.^{21,22} If the hopping rates between microstates, for example, the Arrhenius-type hopping, are further given, then the master equations, which can describe the dynamics of the atomic structure transitions, can be established. The time-series solution of these master equations renders the variation of various physical properties with temperature and time. Although these assumptions seemingly oversimplify the dynamics of an

G. Scherer—contributing editor

Manuscript No. 29223. Received January 25, 2011; approved July 04, 2011.

[†]Author to whom correspondence should be addressed. e-mail: liangchi.zhang@unsw.edu.au

atomic system, the practical result is encouraging. Mauro and Loucks²³ implemented the master equation approach to study the glass transition of selenium and obtained a satisfactory agreement with the experimental result in terms of the volume change in the glass transition range. To efficiently solve the master equations, they²⁴ devised the metabasin technique, through grouping the basins with fast intrabasin hopping rates into a metabasin and by assuming the ergodicity in metabasins, to allow the integration time step to be inversely proportional to the cooling rate, so that the simulation time can be a constant for the cooling rate varying from 10^{12} to 10^{-12} K/s. This approach seems to be practical for calculating various thermodynamic properties, such as molar volume, potential energy, enthalpy, and entropy, for realistic glass-forming systems with an arbitrary thermal history.

This study aims to achieve a much higher simulation efficiency by developing a Monte-Carlo approach to obtain a close approximation to that of the exact solutions of the master equations. In this way, the master equation method can be incorporated into the finite element simulation, so as to deepen the understanding of glass behavior in a prescribed thermo-mechanical process.

II. Master Equations and Approximate Monte-Carlo Solution

(1) Master Equations

Suppose that a PEL or an enthalpy landscape of an atomic system can be described by a countable number of basins with energy minima U_i , the degeneracy factor g_i , and the effective saddles U_{ij} ($U_{ij} = U_{ji}$) between two basins i and j . The hopping rate K_{ij} from basin i to j is assumed to be²⁴

$$K_{ij} = v_0 g_j \exp\left(-\frac{U_{ij} - U_i}{k_B T}\right) \quad (1a)$$

where v_0 is the reference attempting frequency, k_B and T are Boltzmann constant and temperature, respectively. The saddle energy U_{ij} which must be crossed by the hopping $i \rightarrow j$ is difficult to be quantified. Mauro *et al.*²³ assumed that there is a minimum barrier ΔU_i associated with basin i , which may correspond to the rotation or break of atomic bond. They then assumed that²³

$$U_{ij} = \max\{U_i + \Delta U_i, U_j + \Delta U_j\} \quad (1b)$$

More generally, all possible paths for the hopping from basin i to basin j should be considered. The lowest maximum energy among different paths is the critical energy U_{cij} ($U_{cij} = U_{cji}$). The saddle point U_{ij} is then given by

$$U_{ij} = \max\{U_{cij}, U_i + \Delta U_i, U_j + \Delta U_j\} \quad (1c)$$

Dyre²⁵ argued that U_{cij} should be a constant energy U_c based on lattice percolation model. Whereas Doliwa and Heuer²⁶ found that the effective barrier could be linearly related to the basin energy based on their investigation of the average lifetime in a basin. It should be noted that if all basins are reachable without crossing other basins, Eq. (1c) reduces to Eq. (1b).

If the saddle energies have been defined for all possible hopping events, the master equation can be expressed as

$$\dot{f}_i = \sum_{j=1}^N (-f_i K_{ij} + f_j K_{ji}) \quad (2)$$

where $K_{ii} = 0$ and f_i denotes the probability to find the system in basin i and the overhead dot indicates the time

derivative. By letting $L_{ii} = -\sum_{j=1}^N K_{ij}$ and $L_{ij} = K_{ij}$, Eq. (2) can be recast to a matrix form, i.e.,

$$\dot{\mathbf{f}} = \mathbf{f}\mathbf{L} \quad (3)$$

At a high temperature, the hopping rates must be sufficiently large to keep the system in the detailed balance (equilibrium state), which requires:

$$f_i K_{ij} = f_j K_{ji} \quad (4)$$

The steady-state solution of Eq. (4) (i.e., $\dot{\mathbf{f}} = 0 = \mathbf{f}\mathbf{L}$) gives the Boltzmann distribution:

$$\bar{f}_i = g_i \exp\left(-\frac{U_i}{k_B T}\right) / Z \quad (5)$$

where $Z = \sum_{i=1}^N g_i \exp(-U_i/k_B T)$ is the partition function. In a cooling process, the hopping rates K_{ij} reduce exponentially with temperature and the system departs from equilibrium and enters the supercooling region, in which the ergodicity is continuously broken and the viscosity continuously increases. Glass transition temperature is defined at the point where viscosity reaches 10^{12} Pa·s.²⁷ At the temperature much lower than the glass transition point, the detailed balance is not reachable within a finite time period. Therefore, f_i is not a state variable but a history-dependent variable. They have to be determined from Eq. (3), provided that the thermo history starting from a known combination of f_i can be given (e.g., by Eq. (5) at high temperature).

Equation (3) can be numerically solved by a direct Euler Integration (EI) or by an analytical integration, if all eigenvalues and eigenvectors of matrix \mathbf{L} can be accurately determined. An alternative is to use the Gillespie Stochastic Simulation Algorithm (GSSA),²⁸ which can track the detailed time history of every transition event. Nevertheless, these methods are impractical for a system even with only tens of molecules, because the elements of \mathbf{L} vary in many orders of magnitude which either induces significant numerical errors in calculating the eigenvalues or requires an extremely small time step for the direct simulation (i.e., EI and GSSA). In this sense, the Metabasin method proposed by Mauro *et al.*²⁴ becomes appealing due to its efficiency and clear physical ground. However, it is noted that the metabasin approach needs to check the hopping rate between every two basins, leading to a computational complexity of $O(N^2)$ where N is the number of basins. If the number of basins is large, the metabasin approach is still extremely demanding. A new approach which can reduce the computational complexity significantly is therefore necessary. This is described below.

(2) Approximate Monte-Carlo Simulation

Consider a glass transition process represented by the volume-temperature diagram schematically shown in Fig. 1. If the crystallization can be avoided through fast cooling, theoretically one can reduce the cooling rate \dot{T} to obtain an equilibrium curve ABC, along which the detailed balance is retained at every temperature. If the PEL and the volume of each inherent structure are given, this process can be simulated by numerically integrating the master equations. To obtain equilibrium curve ABC, a sufficiently long relaxation time t_{rel} must be given at every temperature. The glass transition along path ABD, which is a deviation from the equilibrium curve ABC, is simply due to the insufficient relaxation time (namely, $\Delta T/\dot{T} < t_{rel}$ where ΔT is the temperature resolution in the simulation). Now, suppose that there is a different description of basin hopping, which can possess one or several adjustable parameters to tune the hopping rates and

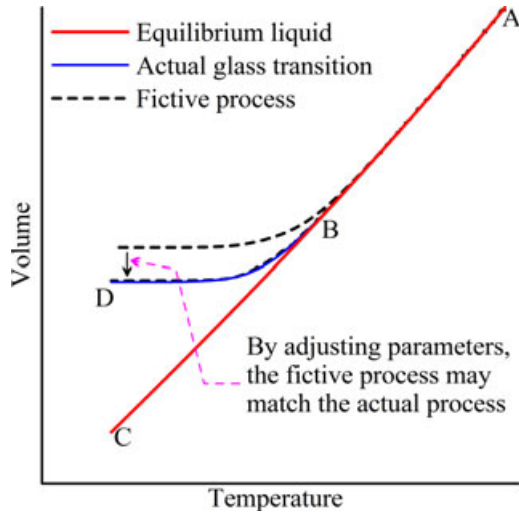


Fig. 1. The volume–temperature diagram of a glass-forming liquid.

to assure the detailed balance (Eq. (4)) at a longtime limit. We can conjecture that this description may be applicable to approximate the actual solution of the master equations. As represented in Fig. 1 by the dashed curves, the fictive hopping process renders another glass transition process for the same cooling rate along curve ABD'. By adjusting the parameters, we expect the dashed curve (fictive process) can match the solid curve (actual process). Conceptually, this is in accord with the phenomenological picture described by Tool⁵ and Narayanaswamy,⁶ but our simplified basin-hopping process to be constructed below will enable the integration of inherent atomic structures.

For convenience, let us call a unit atomic system with known PEL a species. For a macroscopic system composed of M species, $f_i(t)$ is the fraction of species in basin i at time t . We assume that the dynamics of these species does not influence each other (i.e., the factorization hypothesis¹⁹), so that their hopping can be described in a unified way. After Δt , the probability for jumping from basin i to basin j is $P_{ij}(\Delta t)$. A jump normally requires $j \neq i$. But, we may avoid the hassle by defining $P_{ii} = 0$ and let basin j be any basin between 1 and N . This jump includes two stochastic events. The first is the selection of the target basin j , whose probability is denoted by $S_{ij}(\Delta t)$; and the second is the jump, whose probability is denoted by $J_{ij}(\Delta t)$. We then have

$$\begin{aligned} f_i(t + \Delta t) &= f_i(t) \left(1 - \sum_j S_{ij}(\Delta t) J_{ij}(\Delta t) \right) \\ &\quad + \sum_j f_j(t) S_{ji}(\Delta t) J_{ji}(\Delta t) \\ &= f_i(t) - \sum_j [f_i(t) S_{ij}(\Delta t) J_{ij}(\Delta t) - f_j(t) S_{ji}(\Delta t) J_{ji}(\Delta t)]. \end{aligned} \quad (6)$$

At a steady state, $f_i(t + \Delta t) = f_i(t) = \bar{f}_i$. By substituting Eq. (4), the above equation is reduced to

$$\frac{S_{ji}(\Delta t) J_{ji}(\Delta t)}{S_{ij}(\Delta t) J_{ij}(\Delta t)} = \frac{\bar{f}_j}{\bar{f}_i} = \frac{K_{ji}}{K_{ij}} \quad (7)$$

Therefore, any selection and jumping events which satisfy the above equation should render the detailed balance at longtime limit. For simplicity, we assume that (1) the selection is not biased to any basin, namely $S_{ij} = 1/N$; and (2) the jumping probability is

$$J_{ij}(\Delta t) = (1 - \exp(-\beta \lambda_{ij} \Delta t)) \frac{K_{ij}}{\lambda_{ij}} \quad (8)$$

where $\lambda_{ij} = K_{ij} + K_{ji}$ and β is the fitting parameter for matching the simplified stochastic process to the actual solution of the master equations.

The Monte-Carlo algorithm of the above simplified stochastic process is easily implementable. One can use the pseudo-random number generator provided by any computer language to simulate the variation of the M species in a macroscopic system. It is apparent that the computation complexity is $O(M)$ at each time step. As the pseudo-random number has a limited resolution, we shall consider a small number, say 10^{-4} , to be equal to the zero probability in the Monte-Carlo simulation. The detailed algorithm is as follows:

- (1) Give the PEL information, the initial temperature T , initial f_i , cooling or heating rate \dot{T} , Δt , β , and the number of species M .
- (2) For a species k in basin i , generate a random number ξ ($\xi \in [0,1)$); then, the target basin is $j = \text{INT}(N\xi) + 1$ where $\text{INT}(\cdot)$ means integer part.
- (3) Generate another random number ξ , if $\xi < J_{ij}$, the species jumps into basin j and $f_i(t + \Delta t) = f_i(t) - 1/M$, $f_j(t + \Delta t) = f_j(t) + 1/M$.
- (4) $k = k + 1$; if $k \leq M$, go to step (2).
- (5) Update temperature $T = T + \dot{T}\Delta t$, the jumping rates J_{ij} and the time $t = t + \Delta t$.
- (6) Check the completion condition. If not complete, let $k = 1$ and go to step (2).

III. Result and Discussion

(1) Comparison with Other Solutions of Master Equations

We first test the above Monte-Carlo algorithm with a toy system as shown in Fig. 2(a). Suppose the system is balanced at 800 K and then cooled down to 100 K with different cooling rates. The average potential energy is given by $U = \sum_i f_i U_i$. In the Monte-Carlo simulation, we set $M = 10^3$, $\nu_0 = 0.5$ GHz, and $\Delta t = 0.01$ K/ \dot{T} . Figure 2(b) shows the variation of the average potential energy obtained by different approaches. It is noted that when $\beta = 6$, the simplified stochastic process agrees very well with the results of direct integration. The result of metabasin approach²⁴ is also included in Fig. 2(b). The metabasin means the group of basins with relatively small intrabasin barriers [say, the group of basins 4 and 5 as shown in Fig. 2(a)]. Within a metabasin, the intrabasin hopping rates are all larger than the threshold rate λ_{th} (say, $\lambda_{\text{th}}\Delta t = 10$). Therefore, the population within a metabasin can be assumed to be the equilibrium population and the time step for simulating the hopping among different metabasins can be proportional to the cooling rate. At high temperature, all basins are in the single metabasin. With the reduction of temperature, this metabasin splits into multiple metabasins. At a sufficiently low temperature, the metabasins split into basins. The accuracy of the metabasin approach can be controlled by the threshold rate λ_{th} . A larger λ_{th} leads to higher accuracy and longer computational time. However, in our approach, the basin-grouping procedure is discarded as it is time-consuming especially for a large system. Instead, we use Eq. (8) to determine the jumping probability from basin i to basin j within the time step Δt . Based on this equation, for the two adjacent basins with sufficiently large inter-basin hopping rates, the jumping probabilities between them approach time-independent constants. Formally, if $\lambda_{ij}\Delta t$ is sufficiently large, the jumping probability J_{ij} approaches exponentially to a constant K_{ij}/λ_{ij} . In this way, the correlation between adjacent basins is retained. Conversely, if $\lambda_{ij}\Delta t$ is sufficiently small, the jumping probability approaches zero, indicating the loss of correlation. In the following, we only compare our Monte-Carlo model to metabasin approach as the direct integration is not viable for a large system.

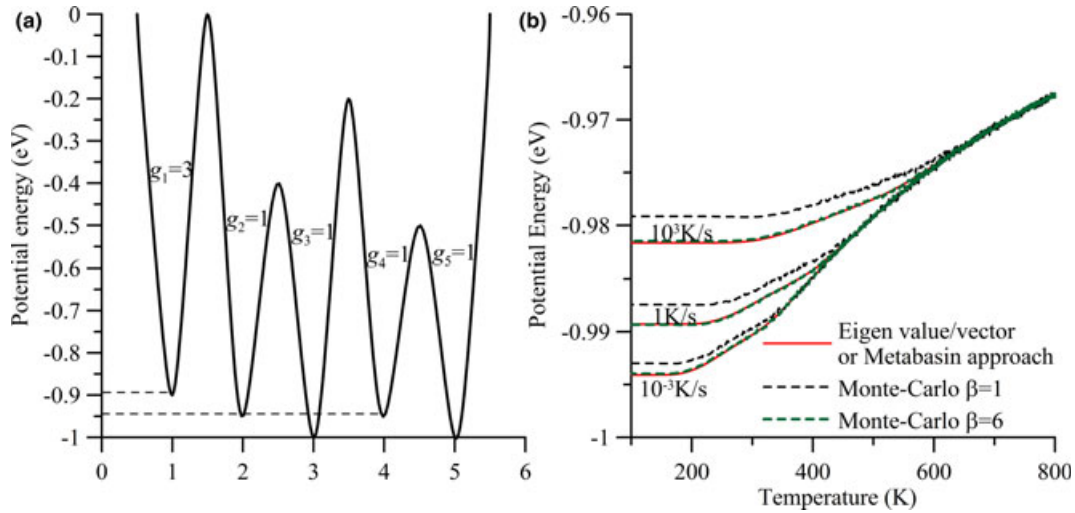


Fig. 2. The solution of master equations of a simple potential energy landscape: (a) the potential energy landscape with five basins; (b) the comparison of different solution methods: for $\beta = 6$, the result of the Monte-Carlo algorithm agrees well with exact and metabasin solutions.

To demonstrate the algorithm for a realistic glass-forming system, we use the data provided by Mauro *et al.*²³ for a system of 64 selenium atoms. Seventy-one unique inherent structures with different enthalpy, degeneracy, and molar volume were identified. The scaling of enthalpy and degeneracy with molar volume is shown in Fig. 3(a). The activation barrier ΔU_i associated with basin i is randomly given at either 1.1 or 0.8 eV. The 1.1 eV barrier occurs twice as frequently as the 0.8 eV barrier. We set $M = 10^4$, $v_0 = 1.4$ THz,²³ and $\Delta t = t_{rel} = 0.01$ K/ \dot{T} . Figure 3(b) compares the results from our algorithm and the metabasin approach in calculating the volume change with temperature for various cooling rates, where V_0 is the molar volume of the equilibrium liquid at 490 K. Excellent agreement is obtained with $\beta = 100$. Figure 3(c) compares the variation of f_i with molar volume at different temperatures, which again shows very good consistency.

We further consider a thermal cycle. Assume, the material is originally at low temperature with the initial constitution identical to the equilibrium state at a fictive temperature T_f , namely, $f_i(t=0) = \bar{f}_i(T_f)$. We heat up the material to a temperature suitable for molding (say, 360 K, viscosity $\approx 10^5$ Pa·s) and then hold for 10 s before cooling down to low temperature (200 K). Figure 3(d) shows the volume change with the temperature for $T_f = 253, 273,$ and 293 K. The good agreement between the metabasin approach and the our Monte-Carlo simulation indicates that our new method can be used to simulate the variations of physical properties of a glass-forming system under a realistic thermal cycle.

(2) Efficiency

The main advantage of the present method is that the computational complexity becomes independent of the basin number N . To verify this, we evenly discretized the curves in Fig. 3(a) into 5000 points for constructing a fictive system. Figure 4 shows the Monte-Carlo simulation result of the cooling curves (cooling rate = 1 K/s) for $M = 10^2, 10^3, 10^4,$ and 10^6 . It is noted that smaller M gives larger fluctuations. However, when $M \geq 10^4$, the fluctuation is minimized and the curves overlap, indicating that $M = 10^4$ is adequate to simulate the macroscopic response of a system characterized by as many as 5000 inherent structures. It should be noted that in case of $N = 5000$, the metabasin approach may need a few days to conduct one simulation of glass transition due to the complexity of $O(N^2)$. Nevertheless, the present Monte-Carlo algorithm only need a few minutes for the same glass transition process with $M = 10^4$.

(3) Determination of β

We introduced β in Eq. (8) to adjust the jumping probability J_{ij} to control the speed of a system approaching its equilibrium state. A larger β leads to the larger jumping probability J_{ij} . For an infinitesimal Δt , $J_{ij} \rightarrow \beta K_{ij} \Delta t$. With $S_{ij} = 1/N$, Eq. (6) reduces to

$$\begin{aligned} \dot{f}_i &= \lim_{\Delta t \rightarrow 0} \frac{f_i(t + \Delta t) - f_i(t)}{\Delta t} \\ &= \sum_j \left[-f_i(t) \frac{\beta}{N} K_{ij} + f_j(t) \frac{\beta}{N} K_{ji} \right] \end{aligned} \quad (9)$$

Therefore, with $\beta = N$ and an infinitesimal Δt , the Monte-Carlo simulation gives the exact solution of the master equations. The incorporation of β is because we defined a two-step hopping in the stochastic process. In the first step, the species should choose a direction to go, which comes with $1/N$ probability (N is the number of basins). This selection step may be probably nonphysical but necessary in computer simulation. We then used $\beta = N$ to remedy this deficiency. For a coarse time series, many hopping events are omitted. β is then used not only to compensate the selection probability but also to artificially increase the hopping rate to approximate the process with infinitesimal Δt . We then assert that $\beta \geq N$ in the simulation. For example, in Fig. 2, as $N = 5$, we used $\beta = 6$ (slightly larger than N) because the Δt cannot be infinitesimal in the computation.

To make the effect of β more transparent, let us consider a simplified system with only two basins 1 and 2 and the equilibrium population $\bar{f}_i = K_{ji}/\lambda_{ij}$ ($i, j = 1, 2,$ and $i \neq j$). Starting from arbitrary $f_i(t_0)$, after one time step Δt , we have

$$\begin{aligned} f_i(t_0 + \Delta t) - \bar{f}_i &= f_i(t_0)(1 - S_{ij}J_{ij}) + f_j(t_0)S_{ji}J_{ji} - \bar{f}_i \\ &= \frac{1 + \exp(-\beta\lambda_{ij}\Delta t)}{2} (f_i(t_0) - \bar{f}_i) \end{aligned}$$

Note that the analytical solution of the master equations of the two-basin system after the relaxation time t_{rel} is $f_i(t_0 + t_{rel}) - \bar{f}_i = \exp(-\lambda_{ij}t_{rel})(f_i(t_0) - \bar{f}_i)$. We then compare the approximate relaxation processes with different β to the analytical solution in Fig. 5. In the calculation, we use a relatively large Δt , that is, $\lambda_{ij}\Delta t = 0.1$. It is noted that with this coarse Δt , $\beta = N = 2$ is not the best choice. A slightly larger β ($= 2.1$) can give rise to a better approximation of the relaxation process.

It is difficult to determine β analytically albeit the above discussion indicates that β is mainly a function of Δt and N .

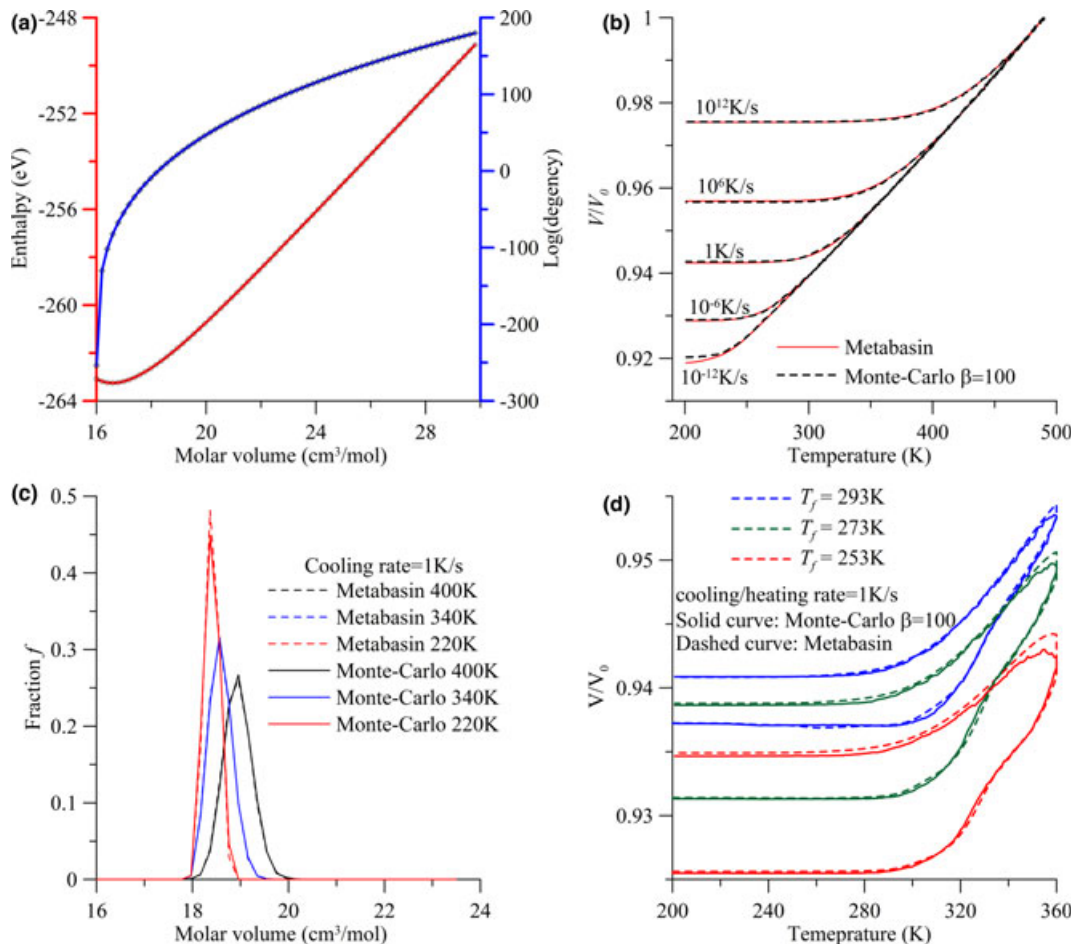


Fig. 3. The simulation of glass transition of a realistic glass-forming system (selenium): (a) the scaling of basin enthalpy and degeneracy with the molar volume of the inheritance structure; (b) the comparison of the volume–temperature curves obtained by the Monte-Carlo simulation and the metabasin approach for different cooling rates; (c) the comparison of the basin visiting probability at three different temperatures for the cooling rate 1 K/s; (d) the comparison of the volume–temperature curves for different thermal cycles.

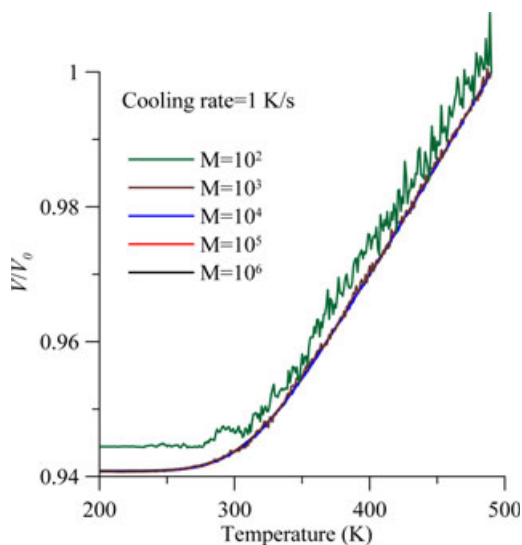


Fig. 4. The convergence of the Monte-Carlo simulation when $M > 10^4$ for a fictive glass-forming system with 5000 basins.

Practically, β is associated with a well-defined thermal process and a suitable Δt ensuring that the simulation can be done within a reasonable duration and is estimated through the comparison of the Monte-Carlo solution to more accurate solutions. For different Δt , different β should be used. In studying the cooling processes with cooling rate varying

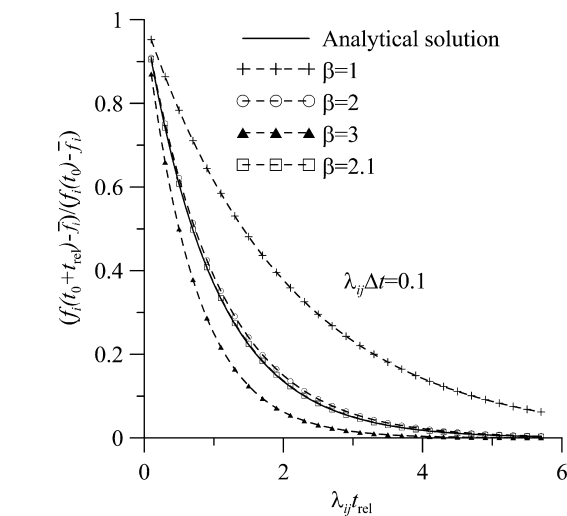


Fig. 5. The comparison of the relaxation process of the two-basin system.

from 10^{12} to 10^{-12} K/s as shown in Fig. 3(b), we used the cooling rate to scale Δt . Then, a single β [$\beta = 100$ in Fig. 3(b)] does not allow Monte-Carlo simulation to match perfectly, all the results of the metabasin approach as shown in Fig. 3(b), although they are very close. Nevertheless, this example also indicates that the system response is not

sensitive to β . Adjusting β is not difficult especially when each Monte-Carlo simulation can be done within several minutes. In our tested examples, β is found to be around $(1-10)N$.

(4) Difference from Kinetic Monte-Carlo Simulation

It should be noted that our algorithm is different from the Kinetic Monte Carlo (KMC) algorithm, which is based on GSSA. We regard KMC as the exact solution to the master equations. In KMC, the selection of the transition path is biased to the fast events, and the time step is a stochastic variable corresponding to the occurrence of one hopping event. The average of time steps is inversely proportional to the sum of the basin hopping rates, which is, however, too small to implement KMC in a macroscale simulations. Our algorithm is an approximate solution, but allows the large prescribed time step. The idea of our algorithm is different from KMC. We do not track exactly every stochastic event in the transition history but only the major events at the specified time steps. We consider that the hopping direction is uniformly toward all basins. Whether this hopping can happen depends on the probability given in Eq. (8), which is just a function of the time step and the forward and backward hopping rates along the selected hopping direction. We ensure by Eq. (9) that the model approaches the exact solution of the master equations if an infinitesimal time step can be used and the population is sufficiently large.

IV. Further Applications

(1) Viscosity

To further implement the Monte-Carlo algorithm to simulate a thermo-mechanical process of a glass-forming system, one should characterize the variation of viscosity with the thermal history. Given the master equations, Mauro *et al.*²⁹ assumed the validity of the Stokes–Einstein relation and expressed the viscosity as

$$\eta_{\text{Mauro}} = DNT \left(\sum_{i=1}^N f_i(T(t)) |L_{ii}| \right)^{-1} \quad (10)$$

where D is a constant related to the average hopping distance of atoms from one basin to another, $|L_{ii}|$ is the total rate for leaving the basin i .

However, the Stokes–Einstein relation actually breaks down at the glass transition range as evidenced by experiments^{30,31} and MD simulations³² and as analyzed by Stillinger and Hodgdon³³ and Taurjus and Kivelson.³⁴ Kushima *et al.*³⁵ and Li³⁶ ascribed the breakdown to the ansatz that the diffusivity is dominated by the fast hopping events, whereas the viscosity is more related to the slow hopping. They envisaged that at a temperature sufficiently lower than the melting temperature, a stress-free macroscopic system can be considered as an ensemble of many microscopic systems. Each microscopic systems has the signature of the basin index i and the residual stress σ_i . The macroscopic stress-free condition requires $\sum_{i=1}^N f_i \sigma_i = 0$. The stress fluctuation of the microscopic system was purely attributed to the basin hopping. Hence, by invoking the Green–Kubo relation, they get³⁶:

$$\eta_{\text{Li}} = \frac{C}{k_B T} \sum_{i=1}^N f_i(T(t)) \sigma_i \sum_j A_{ij}(\omega \rightarrow 0)^{-1} \sigma_j \quad (11)$$

where C is a scaling constant, $A_{ij}(\omega) = \omega \delta_{ij} - L_{ij}$ and σ_i is the residual shear stress of the atomic cluster at basin i which is randomly sampled in $[-1,1]$. We use the Linear Algebra Package LAPACK (<http://www.netlib.org/lapack/>) to solve equations $\sum_j A_{ij} X = \sigma_j$. To reduce the numerical error, we let $A'_{ij} = A_{ij}/L_{ii}$ and solve $\sum_j A'_{ij} X = \sigma_i/L_{ii}$.

For supercooled liquid, the viscosity is considered to be inversely proportional to the characteristic relaxation time.

Adam and Gibbs³⁷ speculated that the system with more possible configurations should have less characteristic relaxation time as it could relax along more trajectories in the phase space. The Adam–Gibbs relation has met with remarkable success in describing the relaxation behavior of a wide variety of systems.⁷ It is formulated as

$$\eta_{\text{AG}} = \eta_0 \exp\left(\frac{Bk_B T_g}{TS_c}\right) \quad (12)$$

where η_0 and B are constants and S_c is the configurational entropy, which is the ensemble average of configurational entropies of individual basins¹⁹:

$$S_c(T(t)) = \sum_{i=1}^N f_i(T(t)) S_{ci} = k_B \left(\sum_{i=1}^N f_i(T(t)) \ln g_i + \ln g_0 \right) \quad (13)$$

We can introduce another parameter g_0 in Eq. (13) because g_i is generally normalized about the estimate of the maximum number of atomic configurations.²³ The exact number of configurations is never known.

The viscosity of selenium has been measured in several ways.^{38,39} We collected those experimental data in Fig. 6(a). In these experiments, the material was annealed at the temperature well above the glass transition temperature for hours prior to the viscosity measurement. We should therefore regard that the material is in equilibrium state and hence $f_i(T(t)) = \bar{f}_i(T)$ in Eqs. (11–13). It is noted that at temperature 305 K, the measured viscosity is about 10^{12} Pa·s.^{38,39} The constants D and C in Eqs. (10) and (11) can then be determined according to this condition. We set $T_g = 305$ K and interpret the viscosity–temperature diagram in the form of the Angell’s plot.²⁷ The calculated curves from Eqs. (10), (11), and (12) were compared in Fig. 6(a) with the experimental data. It is noted that both Eqs. (10) and (11) do not follow the trend of the experimental data. Equation (11) gives good prediction of low-temperature viscosity but fails for high temperature. Nevertheless, Adam–Gibbs relation Eq. (12) excellently fits the experimental data. Therefore, for the present case, we shall resort to the Adam–Gibbs relation as it admirably describes the experimental measurements.

With the parameters η_0 , B , and S_{c0} determined from the viscosity of the equilibrium liquid, let us now consider the viscosity of the nonequilibrium glass obtained with different cooling rates. Figure 6(b) shows that with the decrease of temperature, the viscosity of glass deviates from the equilibrium curve to the iso-configurational (i.e., S_c does not change) curve, which may be termed the fragile-to-strong transition. This transition has also been evidenced in window glass⁴⁰ and in metallic glasses.^{41,42}

(2) Finite Element Simulation

In the finite element simulation, we consider the thermal cycle similar to that shown in Fig. 3(d). The volume change with temperature is embodied by the plastic volumetric strain ε_v^p . The viscous deformation is shear dominant and the Prantl–Reuss relation is used to update the stress field from the elastic response of the material. The constitutive law is specified as

$$\begin{aligned} \dot{\sigma}_{ij} = & 2G \left(\dot{\varepsilon}_{ij} - \frac{1}{3} \delta_{ij} \sum_{k=1}^3 \dot{\varepsilon}_{kk} - \frac{\bar{\tau}}{\eta_{\text{AG}}} \frac{\sigma'_{ij}}{2\bar{\tau}} \right) \\ & + 3K \left(\sum_{k=1}^3 \dot{\varepsilon}_{kk} - \dot{\varepsilon}_v^p \right) \end{aligned} \quad (14a)$$

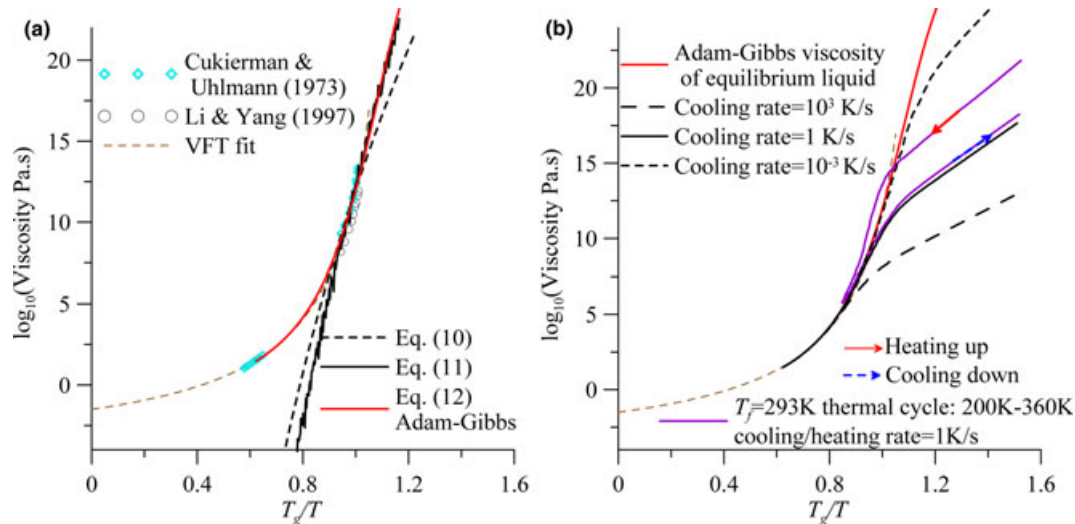


Fig. 6. The viscosity–temperature diagram: (a) the viscosity of equilibrium liquid ($T_g = 305$ K); (b) The viscosity of glass.

$$\sigma'_{ij} = \sigma_{ij} - \frac{1}{3} \sum_{k=1}^3 \sigma_{kk} \delta_{ij} \quad (14b)$$

$$\bar{\tau} = \sqrt{\frac{1}{2} \sum_i \sum_j \sigma'_{ij} \sigma'_{ij}} \quad (14c)$$

where σ_{ij} and ε_{ij} are the stress and strain tensors, respectively; G and K are the shear and bulk modulus; σ'_{ij} and $\bar{\tau}$ are the deviatoric stress tensor and the equivalent shear stress; and the overhead dot denotes the time derivative. A user material subroutine is developed to implement the Monte-Carlo algorithm and the above formula in the finite element analysis. The simulation was conducted with the ABAQUS EXPLICIT solver.

The selenium cylinder as shown in Fig. 7(a) is subjected to the warm compressive molding to form a lens shape as considered by Yi *et al.*¹ For simplicity, we consider the molds to be rigid, the system to be axisymmetric and the heat exchange between the material and its environment to be convective. The mechanical and thermal properties used in the simulation are listed in Table I. Initially, the material is taken out from a refrigerator with initial temperature 200 K and initial constitution identical to the equilibrium state at $T_f = 293$ K (i.e., $f_i(t=0) = f_i(T_f)$). The high temperature (T_H) gas is then purged for t_H seconds to heat up the material with the convective heat transfer coefficient h_H . In the last 10 s of heating stage, the upper mold moves downward at the speed of 0.14 mm/s to compress the gob. After a compression of 10 s, the upper mold is hold still and the low-temperature (T_L) gas is purged to cool the material for t_L seconds with the convective heat transfer coefficient h_L . Finally, we remove the upper mold and investigate the residual stress after the molding process. The parameters T_H , h_H , t_H , T_L , h_L , and t_L used in each simulation are listed in the caption of Fig. 7.

Figure 7(b) is the plot of von Mises stress ($\sqrt{3}\bar{\tau}$) after the compressive molding. It is observed that the residual stress is in the range of 1–20 MPa. As a comparison, if we consider the change of viscosity along the equilibrium curve, the residual stress distribution is similar as shown in Fig. 7(c). This result indicates that the information on the fragile-to-strong transition of viscosity is not significant in evaluating the residual stress resulted from a molding process. The experimentally measured viscosity, which is generally obtained for the equilibrium system, can then be directly applicable. A reduced cooling rate improves the homogeneity of

temperature distribution, which should therefore induce less residual stress. We reduced the convective heat transfer coefficient (h_L) at the cooling stage and increased the cooling time by 10-fold. The result in Fig. 7(d) indicates that the residual stresses can be mitigated to be less than 3 MPa.

In a mass production process, the above large increase in cooling time is undesirable. We should consider a postmolding annealing process to reduce the residual stress. Suppose that after molding, the glass is moved to a furnace with the temperature at 360 K. After keeping the environmental temperature for 60 s, the furnace is cooled down to 200 K in 600 s. The residual stress distribution after annealing is shown in Fig. 7(e). It is noted that the residual stress is randomly redistributed in the material. This randomization is attributed to the stochastic effect of the Monte-Carlo simulation, which makes two elements with identical thermal history have slight different volumes. To mitigate this stochastic effect, one shall refine the mesh and increase M . For the present case, such randomized residual stress distribution should indicate the macroscopic uniformity and the mitigation of residual stress. However, as illustrated in Fig. 3(d), a thermal cycle generally leads to a residual volume change. Therefore, albeit the residual stress is reduced by an order of magnitude, the geometry of the glass product also changes substantially in comparison with Fig. 7(b). To mitigate this geometry change in annealing, the annealing temperature should be reduced. We tried 340 K and present the result in Fig. 7(f), which shows the mitigation of residual stress without notable change of geometry.

V. Concluding Remarks

This study has developed a simple stochastic process to simulate the variations of physical properties in the glass transition process. The corresponding Monte-Carlo algorithm is effective in providing excellent approximation to the exact solutions of master equations. The method is efficient owing to the independency of the basin number. These advantages allow us to incorporate the Monte-Carlo simulation into the finite element simulation of glass molding process, which can offer detailed information of the variation of various physical properties. We have also shown that a reduced cooling rate can effectively reduce the residual stress. However, the significantly increased operation time is undesirable in mass production. An annealing process can be used to reduce the residual stress and to improve the macroscopic uniformity, as an alternative.

The new Monte-Carlo method is applicable to any glass-forming system if the landscape of the potential energy or

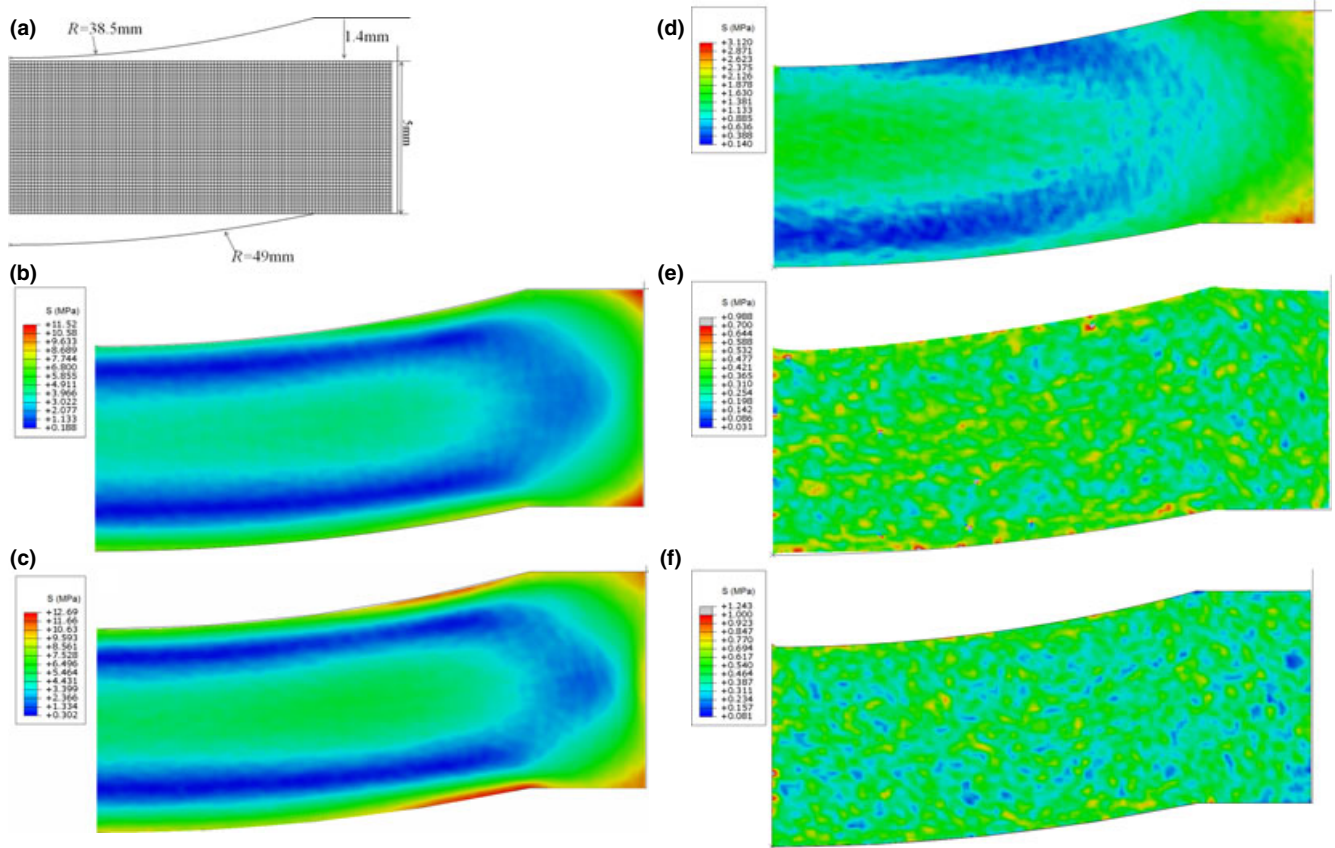


Fig. 7. The finite element simulation of compression molding of selenium: (a) the finite element model and (b–f) the plots of residual stresses after different molding processes with $T_H = 360$ K, $h_H = 100$ W/m²K, $t_H = 60$ s, $T_L = 173$ K, $h_L = 100$ W/m²K; (b) $t_L = 20$ s; (c) $t_L = 20$ s and use the viscosity of equilibrium liquid; (d) $t_L = 200$ s; (e) $t_L = 20$ s and annealed from 360 to 200 K for 600 s; (f) $t_L = 20$ s and annealed from 340 to 200 K for 600 s.

Table I. The Parameters Used in the Monte-Carlo Finite Element Simulation

Name	Symbols	Value	Unit
Bulk modulus	K	8.3	GPa
Shear modulus	G	3.7	GPa
Density		4000	kg·m ⁻³
Thermal conductivity		2	W·(m·K) ⁻¹
Specific heat		0.519	J·(kg·K) ⁻¹
Monte-Carlo parameter	β	100	
Adam–Gibbs fitting parameter	B	150	
Adam–Gibbs fitting parameter	η_0	$10^{-0.7}$	Pa·s
Adam–Gibbs fitting parameter	g_0	e^7	
Glass transition temperature of the equilibrium liquid	T_g	305	K

enthalpy can be quantified. It is of practical importance that the detailed simulation of the glass transition as shown in Section IV allows one to optimize the compression molding process with much reduced experimental efforts.

Particular care is needed when applying our method to describe the change of material properties in glass transition range. The factorization hypothesis is the fundamental assumption of our model, which allows us to simulate the uncorrelated behavior of individual atomic subsystem (namely the species). The macroscopic response of material is

then the average of the responses of M species. For small population, say $M = 100$ in Fig. 4, the average response is notably different from the result of larger M , which demonstrates the difference between small population and large population or concisely the size effect. This size effect is the consequence of stochasticity. Under the factorization hypothesis, if one averages the behaviors of a number of small-population systems, the resulted macroscopic response should still be identical to that of larger population. In our examples, we found that $M > 10^4$ is sufficient for the macroscale simulation.

The factorization hypothesis may fail⁴³ at low temperature due to the increase of dynamic length scales. This size effect may better be interpreted as the coupling effects among species, which is not considered in the present model. To incorporate the coupling effects, the spatial distribution of species and the momentum and energy transfer between species should be considered. In such cases, the temperature will not be the only thermodynamics variable affecting the hopping from one basin to another. It is not clear how to include the coupling effects in the master equations and how significant these effects can be. However, in view of the fact that the hopping among basins is also increasingly difficult as temperature reduces, the effect of coupling on the temperature dependency of some physical properties, for example, the volume or diffusion constant,⁴³ may not be prominent. But for the viscosity, the effect of coupling will be significant as demonstrated by Rehwald *et al.*⁴³

Acknowledgment

The authors thank the Australian Research Council for supporting this research.

References

- ¹A. Y. Yi and A. Jain, "Compression Molding of Aspherical Glass Lenses—A Combined Experimental and Numerical Analysis," *J. Am. Ceram. Soc.*, **88** [3] 579–86 (2005).
- ²J. Schroers, "Processing of Bulk Metallic Glass," *Adv. Mater.*, **22** [14] 1566–97 (2009).
- ³L. Su, Y. Chen, A. Y. Yi, F. Klocke, and G. Pongs, "Refractive Index Variation in Compression Molding of Precision Glass Optical Components," *Appl. Opt.*, **47** [10] 1662–7 (2008).
- ⁴M. D. Ediger, C. A. Angell, and S. R. Nagel, "Supercooled Liquids and Glasses," *J. Phys. Chem.*, **100** [31] 13200–12 (1996).
- ⁵A. Q. Tool, "Relation Between Inelastic Deformability and Thermal Expansion of Glass in Its Annealing Range," *J. Am. Ceram. Soc.*, **29** [9] 240–53 (1946).
- ⁶S. Narayanaswamy, "A Model of Structural Relaxation in Glass," *J. Am. Ceram. Soc.*, **54** [10] 491–8 (1971).
- ⁷G. W. Scherer, "Use of the Adam-Gibbs Equation in the Analysis of Structural Relaxation," *J. Am. Ceram. Soc.*, **67** [7] 504–11 (1984).
- ⁸D. Turnbull and M. H. Cohen, "On the Free-Volume Model of the Liquid-Glass Transition," *J. Chem. Phys.*, **52** [6] 3038–41 (1970).
- ⁹M. H. Cohen and G. S. Grest, "Liquid-Glass Transition, a Free-Volume Approach," *Phys. Rev. B*, **20** [3] 1077–98 (1979).
- ¹⁰A. S. Argon, "Plastic Deformation in Metallic Glasses," *Acta Metall.*, **27**, 47–58 (1979).
- ¹¹F. Spaepen, "A Microscopic Mechanism for Steady State Inhomogeneous Flow in Metallic Glasses," *Acta Metall.*, **25**, 407–15 (1977).
- ¹²J. Jackle, "Models of the Glass Transition," *Rep. Prog. Phys.*, **49** [2] 171–231 (1986).
- ¹³E. Leutheusser, "Dynamical Model of the Liquid-Glass Transition," *Phys. Rev. A*, **29** [5] 2765–73 (1984).
- ¹⁴U. Bengtzelius, W. Götze, and A. Sjölander, "Dynamics of Supercooled Liquids and the Glass Transition," *J. Phys. C Solid State Phys.*, **17** [33] 5915–34 (1984).
- ¹⁵W. Kob, "Computer Simulation of Supercooled Liquids and Glasses," *J. Phys. Condens. Matter*, **11**, 85–115 (1999).
- ¹⁶M. Goldstein, "Viscous Liquids and the Glass Transition: A Potential Energy Barrier Picture," *J. Chem. Phys.*, **51** [9] 3728–39 (1969).
- ¹⁷F. H. Stillinger and T. A. Weber, "Hidden Structure in Liquids," *Phys. Rev. A*, **52** [2] 978–89 (1982).
- ¹⁸F. H. Stillinger and T. A. Weber, "Dynamics of Structural Transitions in Liquids," *Phys. Rev. A*, **28** [4] 2408–16 (1983).
- ¹⁹A. Heuer, "Exploring the Potential Energy Landscape of Glass-Forming Systems: From Inherent Structures via Metabasins to Macroscopic Transport," *J. Phys. Condens. Matter*, **20**, 373101 (2008).
- ²⁰J. C. Mauro, R. J. Loucks, A. K. Varshneya, and P. K. Gupta, "Enthalpy Landscapes and the Glass Transition," *Sci. Model. Simul.*, **15**, 241–81 (2008).
- ²¹F. G. Wang and D. P. Landau, "Efficient, Multiple-Range Random Walk Algorithm to Calculate the Density of States," *Phys. Rev. Lett.*, **86** [10] 2050–3 (2001).
- ²²J. C. Mauro, R. J. Loucks, J. Balakrishnan, and S. Raghavan, "Monte Carlo Method for Computing Density of States and Quench Probability of Potential Energy and Enthalpy Landscape," *J. Chem. Phys.*, **126** [19] 194103 (2007).
- ²³J. C. Mauro and R. J. Loucks, "Selenium Glass Transition: A Model Based on the Enthalpy Landscape Approach and Nonequilibrium Statistical Mechanics," *Phys. Rev. B*, **76** [17] 174202 (2007).
- ²⁴J. C. Mauro, R. J. Loucks, and P. K. Gupta, "Metabasin Approach for Computing the Master Equation Dynamics of Systems with Broken Ergodicity," *J. Phys. Chem. A*, **111** [32] 7957–65 (2007).
- ²⁵J. C. Dyre, "Energy Master Equation: A low Temperature Approximation to Bassler's Random-Walk Model," *Phys. Rev. B*, **51** [18] 12276–94 (1995).
- ²⁶B. Doliwa and A. Heuer, "Hopping in a Supercooled Lennard-Jones Liquid: Metabasins, Waiting Time Distribution, and Diffusion," *Phys. Rev. E*, **67**, 030501 (2003).
- ²⁷C. A. Angell, "Formation of Glasses from Liquids and Biopolymers," *Science*, **267** [5206] 1924–35 (1995).
- ²⁸D. T. Gillespie, "A General Method for Numerically Simulating the Stochastic Time Evolution of Coupled Chemical Reactions," *J. Comput. Phys.*, **22**, 403–34 (1976).
- ²⁹J. C. Mauro, D. C. Allan, and M. Potuzak, "Nonequilibrium Viscosity of Glass," *Phys. Rev. B*, **80** [9] 094204 (2009).
- ³⁰M. T. Cicerone and M. D. Ediger, "Photobleaching Technique for Measuring Ultraslow Reorientation Near and Below the Glass Transition: Tetracene in o-Terphenyl," *J. Phys. Chem.*, **97** [40] 10489–97 (1993).
- ³¹F. Fujara, B. Geil, H. Sillescu, and G. Fleischer, "Translational and Rotational Diffusion in Supercooled Orthoterphenyl Close to the Glass Transition," *Z. Phys. B*, **88**, 195–204 (1992).
- ³²N. P. Lazarev, A. S. Bakai, and C. Abromeit, "Molecular Dynamics Simulation of Viscosity in Supercooled Liquid and Glassy AgCu Alloy," *J. Non-Cryst. Solids*, **353**, 3332–7 (2007).
- ³³F. H. Stillinger and J. A. Hodgdon, "Translation-Rotation Paradox for Diffusion in Fragile Glass-Forming Liquids," *Phys. Rev. E*, **50** [3] 2064–8 (1994).
- ³⁴G. Tarjus and D. Kivelson, "Breakdown of the Stokes-Einstein Relation in Supercooled Liquids," *J. Chem. Phys.*, **103** [8] 3071–3 (1995).
- ³⁵A. Kushima, X. Lin, J. Li, X. F. Qian, J. Eapen, J. C. Mauro, and P. D. S. Yip, "Computing the Viscosity of Supercooled Liquids," *J. Chem. Phys.*, **130** [22] 224504 (2009).
- ³⁶J. Li, A. Kushima, J. Eapen, X. Lin, X. Qian, J. C. Mauro, P. Diep, and S. Yip, "Computing the Viscosity of Supercooled Liquids: Markov Network Model," *PLoS ONE*, **6** [3] e17909 (2011).
- ³⁷G. Adam and J. H. Gibbs, "On the Temperature Dependence of Cooperative Relaxation Properties in Glass-Forming Liquids," *J. Chem. Phys.*, **43** [1] 139–46 (1965).
- ³⁸M. Cukierman and D. R. Uhlmann, "Viscous Flow Behavior of Selenium," *J. Non-Cryst. Solids*, **12**, 199–206 (1973).
- ³⁹F. Yang and J. C. M. Li, "Viscosity of Selenium Measured by Impression Test," *J. Non-Cryst. Solids*, **212**, 136–42 (1997).
- ⁴⁰O. V. Mazurin, Y. K. Startsev, and S. V. Stoljar, "Temperature Dependence of Viscosity of Glass-Forming Substances at Constant Fictive Temperatures," *J. Non-Cryst. Solids*, **105**, 105–14 (1982).
- ⁴¹C. Zhang, L. Hu, Y. Yue, and J. C. Mauro, "Fragile-to-Strong Transition in Metallic Glass-Forming Liquids," *J. Chem. Phys.*, **133** [1] 014508 (2010).
- ⁴²A. I. Taub and F. Spaepen, "The Kinetics of Structural Relaxation of a Metallic Glass," *Acta Metall.*, **28**, 1781–8 (1980).
- ⁴³C. Rehwal, O. Rubner, and A. Heuer, "From Coupled Elementary Ynits to the Complexity of the Glass Transition," *Phys. Rev. Lett.*, **105**, 117801 (2010). □